

NON-EQUILIBRIUM ELECTRONS AND THE SUNYAEV-ZEL'DOVICH EFFECT OF GALAXY CLUSTERS

DOUGLAS H. RUDD

School of Natural Sciences, Institute for Advanced Study, Princeton, NJ 08540 USA

AND

DAISUKE NAGAI

Department of Physics, Yale University, New Haven, CT 06520 and
Yale Center for Astronomy & Astrophysics, Yale University, New Haven, CT 06520
The Astrophysical Journal Letters, accepted

ABSTRACT

We present high-resolution cosmological hydrodynamic simulations of three galaxy clusters employing a two-temperature model for the intracluster medium. We show that electron temperatures in cluster outskirts are significantly lower than the mean gas temperature, because Coulomb collisions are insufficient to keep electrons and ions in thermal equilibrium. This deviation is larger in more massive and less relaxed systems, ranging from 5% in relaxed clusters to 30% for clusters undergoing major mergers. The presence of non-equilibrium electrons leads to significant suppression of the SZE signal at large cluster-centric radius. The suppression of the electron pressure also leads to an underestimate of the hydrostatic mass. Merger-driven, internal shocks may also generate significant populations of non-equilibrium electrons in the cluster core, leading to a 5% bias on the integrated SZ mass proxy during cluster mergers.

Subject headings: galaxies:clusters:general - intergalactic medium

1. INTRODUCTION

In current theories of cosmological structure formation, the cold dark matter and baryon fluid undergoes gravitational collapse, leading to virialized filaments and roughly spherical “halos” on a variety of scales. Collisionless shocks play a critical role in this process by converting the kinetic energy of in-falling baryonic material to thermal energy. This heating leads to large reservoirs of $T = 10^6 - 10^8$ K gas that fills and surrounds massive structures, directly tracing the formation and evolution of cosmic structure.

Observational probes of this gas are generally sensitive only to the electron component of the plasma. Typically, theoretical studies assume that the electrons are in thermal equilibrium with the surrounding ions. However, this is not a good approximation in the low-density outskirts of galaxy clusters due to the extended timescale for electrons to reach equilibrium via Coulomb collisions (Fox & Loeb 1997; Ettori & Fabian 1998). In the pre-shock intergalactic medium, the bulk of the kinetic energy is carried by the heavier ions. Since the electrons and ions are only weakly coupled, this leads to an electron temperature in the post-shock plasma that is significantly lower than that of ions. The post-shock electrons and ions gradually relax to a single equilibrium temperature.

The low emissivity of gas at densities of $10^{-4} - 10^{-5}$ cm⁻³ has heretofore limited X-ray spectroscopic temperature measurements to regions where electrons are expected to have reached equilibrium (Markevitch et al. 1998; Vikhlinin et al. 2005; Pratt et al. 2007). Advances in the sensitivity of X-ray instruments are pushing the limit of ICM temperature measurements to a significant fraction of the virial radius (e.g., George et al. 2009). Such measurements remain expensive with the current generation of instruments, however.

In recent years the thermal Sunyaev Zel'dovich effect (SZE) has been suggested as a possible probe of gas in this phase (e.g., Afshordi et al. 2007; Hallman et al. 2007, 2009), due to its weaker density dependence. Observations using the next generation of SZ experiments are ongoing, and are expected

to provide accurate measurements of the electron pressure beyond the virial radius. Large samples of massive clusters with profile measurements beyond the virial radius should therefore become available in the near future.

In this work we consider the impact of the two-temperature structure of the intracluster medium (ICM) on the thermal SZE. We employ high resolution simulations of clusters which improve on previous studies (Takizawa 1999; Chieze et al. 1998; Courty & Alimi 2004; Yoshida et al. 2005; Yoshikawa & Sasaki 2006) by combining the efficient shock-capturing properties of Eulerian adaptive mesh refinement with high mass and spatial resolution such that both the large-scale accretion shocks and internal, merger-driven shocks are well captured. We show that the lower electron temperature in the cluster outskirts leads to a significant underestimate of the gas pressure when derived through the SZE. We also demonstrate that the two-temperature structure of the ICM is sensitive to recent accretion history through internal merger-driven shocks and discuss the relative importance of these shocks to the SZE.

2. TWO TEMPERATURE COSMOLOGICAL CLUSTER SIMULATIONS

The simulations were performed using the ART code (Kravtsov et al. 1997, 2002), which was modified to model a two temperature electron-ion plasma. Following Yoshida et al. (2005), we divide the plasma into two components, electrons and ions, which are assumed to be individually in local thermodynamic equilibrium (LTE) with separate Maxwellian velocity distributions defined by temperatures T_e and T_i , respectively. The separation into only two species, electrons and ions, each in separate equilibrium is reasonable, since the self-equilibration timescales for each specie, t_{ii} and t_{ee} , are considerably shorter than the electron-ion equilibration timescale, t_{ei} (Fox & Loeb 1997; Spitzer 1962).¹ When an electron-ion plasma passes through a shock, most of the kinetic energy

¹ $t_{ei} \sim (m_i/m_e)^{1/2} t_{ii} \sim (m_i/m_e) t_{ee}$.

TABLE 1
LIST OF SIMULATED CLUSTERS

Name ¹	r_{200} (h^{-1} Mpc)	M_{200} ($10^{14}h^{-1}$ Mpc)	T_m^2 (keV)	Dynamical state ³ (Rel/Unrel)
CL101 ..	1.77	12.83	6.40	Unrelaxed
CL104 ..	1.42	6.69	5.44	Relaxed
CL6	0.95	1.98	2.14	Relaxed

¹ Cluster labels correspond to those used in Nagai et al. (2007a).

² T_m is the gas-mass weighted temperature measured within r_{200} .

³ Classification of dynamical state is described in Nagai et al. (2007b).

goes into heating the heavier ions, causing $T_i \gg T_e$. After the shock, electrons and ions slowly equilibrate via Coulomb interactions, each converging to the mean gas temperature, $T_{\text{gas}} = (n_e T_e + n_i T_i) / (n_e + n_i)$, over a typical electron-ion equilibration timescale, t_{ei} . The evolution of the electron temperature is given by,

$$\frac{dT_e}{dt} = \frac{T_i - T_e}{t_{ei}} - (\gamma - 1)T_e (\nabla \cdot \mathbf{v}), \quad (1)$$

where the second term accounts for adiabatic compression heating and cooling. The timescale for equipartition between two charged species is given by Spitzer (1962),

$$t_{eq} = \frac{3m_1 m_2}{8(2\pi)^{1/2} n_2 Z_1^2 Z_2^2 e^4 \ln \Lambda} \left(\frac{kT_1}{m_1} + \frac{kT_2}{m_2} \right)^{3/2}, \quad (2)$$

where m , T , and Z are the mass, temperature, and charge of each specie, respectively, n is the number density, and $\ln \Lambda \approx 40$ is the Coulomb logarithm. For the fully ionized ICM, including contributions from both protons and He^{++} , the timescale for equilibration is,

$$t_{ei} \approx 6.3 \times 10^8 \text{ yr} \frac{(T_e / 10^7 \text{ K})^{3/2}}{(n_i / 10^{-5} \text{ cm}^{-3}) (\ln \Lambda / 40)}. \quad (3)$$

Note that this timescale can be comparable to the Hubble time in regions with $T \sim 10^7$ K and overdensities 10 – 100 with respect to the cosmic mean.

While our model assumes negligible electron heating within shocks, some non-adiabatic heating due to plasma instabilities is likely. However, theoretical expectations for the amount and source of electron heating in these shocks vary widely (see, e.g., Bykov et al. 2008, for a recent review), ranging from a constant fraction $T_e \sim 0.2T_i$ of the pre-shock kinetic energy (Cargill & Papadopoulos 1988) to a constant post-shock electron temperature and inverse-square scaling with shock velocity $T_e/T_i \sim v_s^{-2}$ (Ghavamian et al. 2007). In either case we expect the electron heating in the high Mach number accretion shocks to be small. There are some indications of more rapid electron equilibration in shocks with lower Mach number in the ICM (Markevitch 2006), however, the process is not yet well constrained by observations to date. We therefore neglect it in our model, noting that our results represent a maximum of the possible effect.

In this work we re-simulate three galaxy clusters selected from the sample presented in Nagai et al. (2007a, N07 hereafter). The initial conditions and simulation parameters are identical to N07, except the simulations we present here neglect the physics of radiative cooling and star formation, which should have negligible impact in the cluster outskirts. The cluster properties at $z = 0$ are summarized in Table 1. These clusters are chosen to cover a range of mass and the

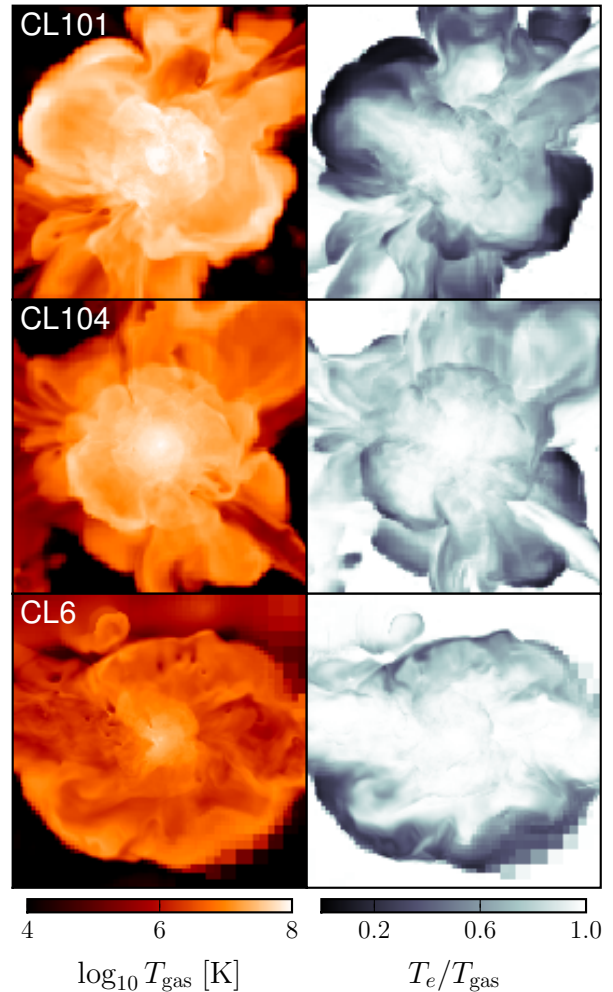


FIG. 1.— The distribution of the mean gas temperature (T_{gas}) and the ratio of electron and mean gas temperatures (T_e/T_{gas}) for three simulated clusters at $z = 0$. *Left panel:* the projected mass-weighted gas temperature in $1h^{-1}$ Mpc slices centered on each cluster and $12h^{-1}$ Mpc on a side. *Right panel:* the ratio of the electron-temperature T_e to the mean ICM temperature T_{gas} .

dynamical histories. CL101 is a massive, dynamically active cluster, which experiences violent mergers at $z \sim 0.1$ and $z \sim 0.25$. CL104 is a similarly massive cluster, but with a more quiescent history. This cluster has not experienced a significant merger for the past 6 Gyrs, making it one of the most relaxed systems in the N07 sample. The last cluster in our sample, CL6, is a fairly relaxed, low-mass cluster at $z = 0$, but experiences a nearly equal mass major merger at $z = 0.6$. Each cluster is simulated using a 128^3 uniform grid with 8 levels of refinement. CL101 and CL104 are selected from $120h^{-1}$ Mpc computational boxes and CL6 is selected from a $80h^{-1}$ Mpc box, achieving peak spatial resolution of $\approx 3.6h^{-1}$ kpc and $\approx 2.4h^{-1}$ kpc, respectively. The dark matter particle mass in the region surrounding the cluster is $9 \times 10^8 h^{-1} M_\odot$ for CL101 and CL104 and $3 \times 10^8 h^{-1} M_\odot$ for CL6, while the rest of the simulation volume is followed with lower mass and spatial resolution.

3. RESULTS

Figure 1 illustrates the complex and highly aspherical distributions of gas temperature (*left panel*) and non-equilibrium electrons (*right panel*) in the outskirts of the simulated galaxy

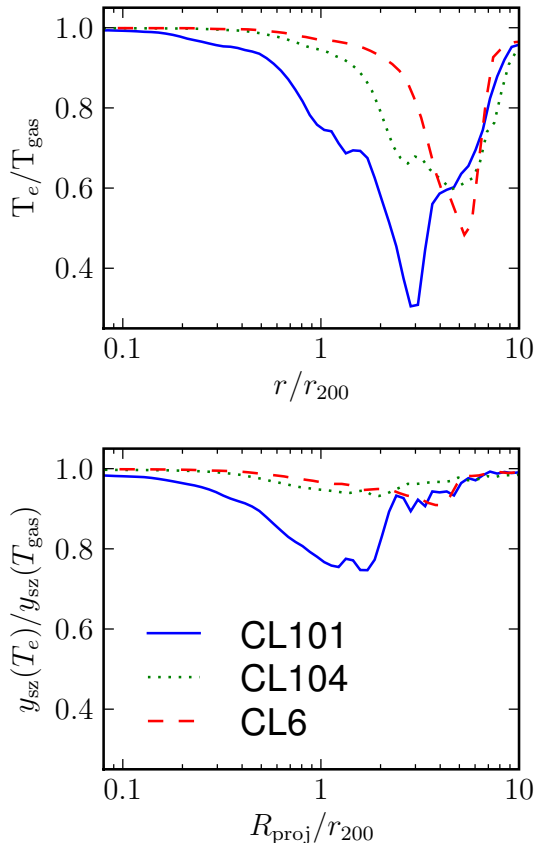


FIG. 2.— Profiles of ICM electron temperature relative to the mean ICM gas temperature for each cluster at $z = 0$. *Top panel:* 3D electron temperature profiles plotted averaged in spherical shells and scaled to r_{200} . *Bottom Panel:* 2D mass-weighted electron temperature profiles averaged in cylindrical annuli projected $60h^{-1}$ Mpc through the simulation volume. This quantity is equivalent to the bias in the observed SZ flux in each annulus with respect to the flux one would observe if the electron temperature, T_e , were equal to the mean gas temperature, T_{gas} .

clusters at $z = 0$. These maps highlight a complicated network of non-equilibrium electrons associated with accreting and shocked material. The recent mergers in CL101 generate both internal and external shocks, and these shocks are responsible for the significant quantity of non-equilibrium electrons throughout the cluster. Non-equilibrium electrons are found mostly in the cluster outskirts for the relaxed systems (CL104 and CL6), and electrons and ions in the inner regions are mostly in equilibrium.

The top panel of Figure 2 shows the spherically averaged 3D radial profile of T_e/T_{gas} as a function of the cluster-centric radius for the simulated clusters at $z = 0$. For the relaxed clusters, electrons and ions are in nearly perfect thermal equilibrium within $r = 0.5r_{200}$. Beyond this radius, the electron temperature becomes increasingly smaller than the mean gas temperature, and the magnitude of the bias is inversely proportional to the ICM temperature: T_e is biased low by 5% at $r = r_{200}$ for CL104 and $r = 2r_{200}$ for CL6. The bias reaches its maximum at the virial shock, $r_{\text{shock}} = [5 - 6]r_{200}$. Beyond the shock radius, electrons and ions in the unshocked gas are largely in equilibrium, with a slight departure from equilibrium due to the accretion shocks of large-scale filaments.

The magnitude of the non-equipartition between electrons

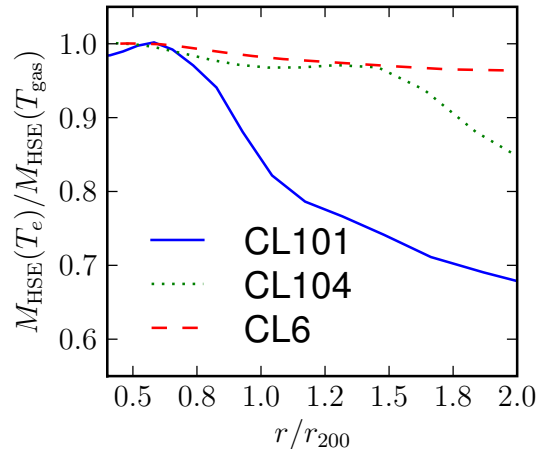


FIG. 3.— The bias in the hydrostatic mass estimate of galaxy clusters due to the non-equipartition of electrons and ions. The bias is defined as the difference in the hydrostatic masses computed using the electron temperature and the mean gas temperature.

and ions depends sensitively on the cluster dynamical state. The largest deviation from thermal equilibrium is seen in the most massive and least relaxed system (CL101). For this cluster, we find $T_e/T_{\text{gas}} \approx 0.75 - 0.9$ at relatively small radii $r = [0.5 - 1]r_{200}$ and reaching a minimum $T_e/T_{\text{gas}} \approx 0.35$ at $r = 3r_{200}$. The non-equilibrium electrons at small radius are primarily generated by internal shocks associated with the recent merger (see also Figure 1).

Production of non-equilibrium electrons by internal shocks within the virialized regions of clusters is illustrated in Figure 4, which shows the evolution of T_e/T_{gas} for CL6 during the period immediately following a nearly equal mass merger around $z = 0.6$ (see also Figures 1 and 2 in Nagai & Kravtsov 2003). The final coalescence generates a strong internal shock which propagates out from the cluster center exciting a thin, trailing layer of non-equilibrium electrons. Although at fixed radius this is a transient phenomenon, lasting for only about $10^7 - 10^8$ yrs due to the short equilibration timescale within the high-density ICM, the shock propagation occurs on a dynamical timescale. This leads to non-equilibrium electrons in the cluster center for 0.5–1 Gyr during the merger. These internal shocks can therefore introduce a significant temperature bias on considerably smaller scales than the accretion shocks.

The suppression of the electron temperature also leads to a bias in the hydrostatic mass estimate, $M_{\text{HSE}}(< r) \propto -dP/dr$, as shown in Figure 3. We follow the procedure described in Lau et al. (2009) for computing the hydrostatic mass profiles. Briefly, we reduce spurious fluctuations in the numerical derivatives by removing gas in bound substructures and then smooth the resulting profile with a Savitzky-Golay filter. At small scales, $r \lesssim 0.7 r_{200}$, the deviation from the hydrostatic mass estimated using T_{gas} is small for all three clusters, and remains $\lesssim 5\%$ for the relaxed clusters out to $1.5 r_{200}$. The bias in the hydrostatic mass is quite large for clusters undergoing recent major mergers (e.g., CL101), where the hydrostatic mass is underestimated by 20–30% in the radial range $[1 - 2] r_{200}$. Note that this effect is in addition to the bias introduced by the non-thermal pressure due to random gas motions (Lau et al. 2009).

These biases in temperature due to non-equilibrium electrons have important implications for the interpretation of Sunyaev-Zel'dovich effect (SZE) observations. This is illustrated in the bottom panel of Figure 2, which shows that the

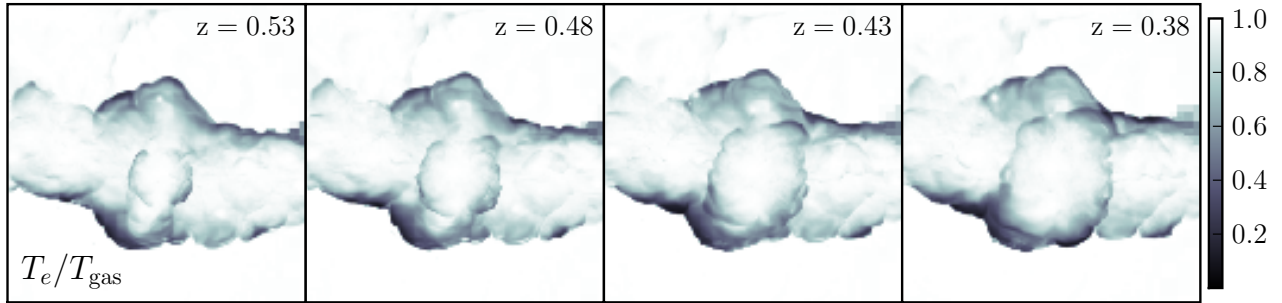


FIG. 4.— The evolution of T_e/T_{gas} surrounding CL 6 from $z = 0.53$ to $z = 0.38$. This cluster experiences a major merger at $z \sim 0.6$, which is nearly in the plane of the figure. This merger causes symmetric merger shocks which propagate outward from the center, eventually reaching and merging with the cluster virial shock at $z \sim 0.3$.

presence of non-equilibrium electrons leads to significant suppression of the SZE signal at large cluster-centric radius. We define the bias to be the ratio of the Compton- y parameters, defined as $y_{\text{SZ}}(T) \equiv \int n_e T dl$, computed alternately using T_e and T_{gas} . Again the bias is largest for the unrelaxed system, and is as large as 20% in the radial range $[0.7 - 2]r_{200}$. The bias is more moderate (5 – 10%) for the other two relaxed systems in a similar radial range.

The integrated Compton- y parameter, Y_{SZ} (or SZ flux), is also affected by the non-equilibrium electrons. But, the biases are much smaller since the effect is averaged over the entire cluster and is dominated by the central regions where electrons are in equilibrium. Examining the evolution of the bias in Y_{SZ} within the spherical region of r_{500} for all three simulated clusters, we find the bias is no larger than 6%, which occurs during periods of major mergers (e.g., CL101 since the last major merger at $z \sim 0.1$ or CL6 at $z \sim 0.6$ as shown in Fig 4). The bias reaches 9% during the same period when measured within the larger radius, r_{200} . This process may also affect the scatter in the mass-observable relations. At various times during the last CL101 merger, however, the cluster lies both above and below the mean Y-M relation, while the bias due to non-equilibrium electrons always acts to suppress the SZ signal. Large samples of simulated clusters are therefore needed to adequately address this effect. For comparison, we computed the bias in X-ray spectroscopic temperature using the *spectroscopic-like* formula of Mazzotta et al. (2004). The resulting bias is negligible, even during mergers, since it is strongly weighted to gas at higher densities and correspondingly shorter t_{ei} .

4. CONCLUSIONS

We use simulations of cosmological cluster formation to explore the two temperature structure of the ICM and its effects on the Sunyaev-Zel'dovich effect. We show that electron temperatures are lower than the ion (or mean gas) temperature in the low-density outskirts of galaxy clusters, where Coulomb collisions are insufficient to keep electrons and ions in thermal equilibrium. This leads to a decrease in the SZE relative

to predictions which assume electron-ion equilibrium. The suppression of electron pressure in turn leads to an underestimate of the hydrostatic mass.

Our simulations also show that the magnitude of the non-equipartition between electrons and ions depends sensitively on the cluster dynamical state. The electron temperature (or pressure) is smaller than the mean gas temperature by about 5% at $r = r_{200}$ for relaxed clusters, but the bias could be as large as 30% for unrelaxed systems, in which populations of non-equilibrium electrons are created within the virial regions of cluster by internal, merger-driven shocks. Although these are short-lived in the high-density ICM, these non-equilibrium electrons can affect global properties, such as the integrated Compton- y or the mass weighted temperature, by about 5%. X-ray spectroscopic temperature, on the other hand, is not significantly affected even during the merger periods, since it is strongly weighted to gas at higher densities and correspondingly shorter t_{ei} . These biases are the sources of systematic uncertainties that will need to be taken into account for the interpretation of upcoming large-scale SZE experiments, including ACT², Planck³, and SPT⁴.

We lastly note that the details of electron equilibration will affect the ability to detect virial shocks using the SZ (Kocsis et al. 2005; Molnar et al. 2009) by smoothing the electron temperature profile in the region of the shock. Successful detections of accretion shocks by ALMA⁵ can be used to place strong constraints on the otherwise uncertain physics operating at these shocks. We will explore this possibility in an upcoming paper.

We thank Kevin Heng for helpful discussions during early stages of this work, Erwin Lau for providing his code to measure the hydrostatic mass, and Fang Peng for useful comments on the manuscript. DHR gratefully acknowledges the support of the Institute for Advanced Study. The simulations were performed at the Joint Fermilab - KICP Supercomputing Cluster, supported by grants from Fermilab, Kavli Institute for Cosmological Physics, and the University of Chicago.

² Atacama Cosmology Telescope (<http://www.physics.princeton.edu/act/>)

³ Planck Surveyor (<http://planck.esa.int/>)

⁴ South Pole Telescope (<http://pole.uchicago.edu>)

⁵ Atacama Large Millimeter Array (<http://www.alma.nrao.edu/>)

REFERENCES

- Cargill, P. J. & Papadopoulos, K. 1988, ApJ, 329, L29
Chieze, J.-P., Alimi, J.-M., & Teyssier, R. 1998, ApJ, 495, 630
Courty, S. & Alimi, J. M. 2004, A&A, 416, 875
Ettori, S. & Fabian, A. C. 1998, MNRAS, 293, L33
Fox, D. C. & Loeb, A. 1997, ApJ, 491, 459
George, M. R., Fabian, A. C., Sanders, J. S., Young, A. J., & Russell, H. R. 2009, MNRAS, 395, 657
Ghavamian, P., Laming, J. M., & Rakowski, C. E. 2007, ApJ, 654, L69
Hallman, E. J., O'Shea, B. W., Burns, J. O., Norman, M. L., Harkness, R., & Wagner, R. 2007, ApJ, 671, 27
Hallman, E. J., O'Shea, B. W., Smith, B. D., Burns, J. O., & Norman, M. L. 2009, ArXiv e-prints
Kocsis, B., Haiman, Z., & Frei, Z. 2005, ApJ, 623, 632
Kravtsov, A. V., Klypin, A., & Hoffman, Y. 2002, ApJ, 571, 563
Kravtsov, A. V., Klypin, A. A., & Khokhlov, A. M. 1997, ApJS, 111, 73
Lau, E. T., Kravtsov, A. V., & Nagai, D. 2009, ArXiv e-prints
Markevitch, M. 2006, in ESA Special Publication, Vol. 604, The X-ray Universe 2005, ed. A. Wilson, 723
Markevitch, M., Forman, W. R., Sarazin, C. L., & Vikhlinin, A. 1998, ApJ, 503, 77
Mazzotta, P., Rasia, E., Moscardini, L., & Tormen, G. 2004, MNRAS, 354, 10
Molnar, S. M., Hearn, N., Haiman, Z., Bryan, G., Evrard, A. E., & Lake, G. 2009, ApJ, 696, 1640
Nagai, D. & Kravtsov, A. V. 2003, ApJ, 587, 514
Nagai, D., Kravtsov, A. V., & Vikhlinin, A. 2007a, ApJ, 668, 1
Nagai, D., Vikhlinin, A., & Kravtsov, A. V. 2007b, ApJ, 655, 98
Pratt, G. W., Böhringer, H., Croston, J. H., Arnaud, M., Borgani, S., Finoguenov, A., & Temple, R. F. 2007, A&A, 461, 71
Spitzer, L. 1962, Physics of Fully Ionized Gases
Takizawa, M. 1999, ApJ, 520, 514
Vikhlinin, A., Markevitch, M., Murray, S. S., Jones, C., Forman, W., & Van Speybroeck, L. 2005, ApJ, 628, 655
Yoshida, N., Furlanetto, S. R., & Hernquist, L. 2005, ApJ, 618, L91
Yoshikawa, K. & Sasaki, S. 2006, PASJ, 58, 641